fermentation

MDPI

Article

Thermotolerant *Cyberlindnera jadinii* Acquired by Adaptive Laboratory Evolution on Ethanol–Acetate for Improved Single-Cell Protein Production

Limei Chen [1,2], Liucheng Long [2], Xizhen Liu [2], Wenqin Bai [2], Yixin Cao [2], Bingxuan Liu [1], Guanyi Chen [1,3], Beibei Yan [1,*] and Demao Li [2,*]

[1] School of Environmental Science and Engineering, Tianjin University, Tianjin 300072, China; chen_lm@tib.cas.cn (L.C.); chen@tju.edu.cn (G.C.)
[2] Tianjin Key Laboratory for Industrial Biological System and Bioprocessing Engineering, Tianjin Institute of Industrial Biotechnology, Chinese Academy of Sciences, Tianjin 300308, China
[3] School of Mechanical Engineering, Tianjin University of Commerce, Tianjin 300134, China
* Correspondence: yanbeibei@tju.edu.cn (B.Y.); li_dm@tib.cas.cn (D.L.); Tel.: +86-(022)-84861993 (D.L.)

Abstract

To obtain thermotolerant *Cyberlindnera jadinii* strains with high-efficiency utilization of ethanol–acetate carbon sources, serial-batch-transfer adaptive laboratory evolution (ALE) under 37 °C was performed on the wild-type strain *C. jadinii* TU389, and a thermotolerant evolved strain *C. jadinii* X131 was acquired. Results demonstrated that *C. jadinii* X131 exhibited superior biomass accumulation compared to the wild-type strain at both the optimal temperature of 31 °C and 37 °C. Specifically, the X131 strain showed 43.4% higher biomass and 45.1% higher protein yield than wild-type strain at 37 °C in 5 L fermenters, with complete amino acid composition, high amino acid score and relative coefficient. Transcriptomic analysis indicated that temperature ALE reprogrammed ethanol oxidation from the cytoplasm to mitochondria to realize in situ detoxification of acetaldehyde, comprehensively activated DNA replication, chromosome segregation, and chromatin remodeling pathways to sustain cell cycle progression under high temperature, and simultaneously reduced peroxisomal metabolic load and redundant transport pathways. *C. jadinii* X131 can efficiently utilize ethanol–acetate carbon sources without adaptive trade-offs, which reduces cooling energy consumption in industrial fermentation.

Keywords: *Cyberlindnera jadinii*; serial-batch-transfer adaptive laboratory evolution; transcriptome; alcohol dehydrogenase; aldehyde dehydrogenase; single-cell protein; thermotolerance; ethanol and acetate carbon source

Check for updates

Academic Editor: Massimo Iorizzo

Received: 22 August 2026
Revised: 5 October 2026
Accepted: 5 October 2026
Published: 14 October 2026

Copyright: © 2026 by the authors. Licensee MDPI, Basel, Switzerland. This article is an open access article distributed under the terms and conditions of the Creative Commons Attribution (CC BY) license.

1. Introduction

Cyberlindnera jadinii, previously classified as *Candida utilis*, is a safe and efficient eukaryotic single-cell microbe with broad carbon source utilization spectrum, high protein synthesis capacity, and non-pathogenicity [1]. It has been widely applied in food fermentation, feed additive production, bioenergy development, and environmental pollutant remediation [2], especially exhibiting unique advantages in single cell protein production and resource recycling of organic wastes [3,4].

Industrial fermentation processes commonly expose microorganisms to multiple adverse stresses including high-temperature, substrate limitation, and product inhibition,

among which high temperature stress acts as a critical bottleneck restricting fermentation efficiency and strain stability. High temperature not only reduces enzymatic activity, increases cell membrane permeability, and triggers excessive accumulation of reactive oxygen species (ROS) [5], but also disrupts genome-stability-related pathways and cell cycle progression, ultimately leading to significant declines in microbial biomass and product synthesis efficiency. These defects severely limit the large-scale industrial application of *C. jadinii*. Previous studies have confirmed that 31 °C is the optimal temperature for biomass and protein accumulation of *C. jadinii* [6], while growth is markedly inhibited and biomass drops sharply at temperatures above 37 °C [7,8], restricting its application in high-temperature fermentation systems such as open-air summer fermentation and high-temperature industrial wastewater treatment.

Ethanol and acetic acid are typical by-products generated during industrial fermentation (e.g., brewing and bioethanol production from syngas [9–11] and organic waste degradation), serving as low-cost and renewable carbon sources. Ethanol acts as an ideal electron donor for carbon chain elongation [12] and energy supply in microorganisms [13], and synergistic utilization of ethanol and acetic acid achieves efficient resource recycling. Using ethanol and acetic acid as the sole carbon sources for microbial fermentation can effectively reduce fermentation costs, realize waste resource utilization [14], and alleviate substrate competition and cost pressure caused by traditional carbon sources such as glucose and maltose, possessing great industrial application prospects [4]. However, syngas fermentation by *Clostridium autoethanogenum*, which supplies the potential carbon source of ethanol–acetate feedstock for future use, is operated at 37 °C. Thus, obtaining a *C. jadinii* strain that grows efficiently at 37 °C would allow direct thermal coupling of the two fermentation stages and avoid the energy penalty of cooling the 37 °C effluent to the wild-type *C. jadinii* optimum of ~31 °C.

Serial-batch-transfer adaptive laboratory evolution (ALE) imposes controlled environmental stress to select strains with heritable phenotypic improvement. This approach has been widely used for stress resistance modification of yeasts including *Saccharomyces cerevisiae* [15,16]. Existing studies have reported that *C. jadinii* resists selenium stress by accumulating trehalose and glycogen for metabolic defense [17], whereas no research has focused on the high-temperature domestication of *C. jadinii* using ethanol–acetate as the sole carbon source.

Transcriptome sequencing has been extensively applied in mechanistic research on non-conventional yeasts. Current transcriptomic studies on *C. jadinii* mainly focus on stress response mechanisms (uranium and selenium stress) [18], metabolic adaptation for heterologous protein expression (zein production) [19], molecular regulatory networks underlying fermentation with unconventional substrates (cottonseed hull) [20], and metabolic regulation of acetaldehyde dehydrogenase [4]. These studies have verified the robust free radical scavenging, DNA damage repair, and metabolic and detoxification capabilities of *C. jadinii* as an efficient cell factory. Recent integrated genomic and transcriptomic analysis revealed mixed ploidy (diploid and triploid) in *C. jadinii* populations, with triploid strains exhibiting stronger environmental stress adaptation at the transcriptional level, which revises the basic parameters for metabolic flux simulation based on transcriptomic data [21].

The present work performed serial-batch-transfer ALE under 37 °C with ethanol–acetate as sole carbon source to obtain thermotolerant evolved *C. jadinii*. The growth characteristics of the evolved and wild-type strains at 31 °C and 37 °C were systematically evaluated. Furthermore, transcriptome sequencing was performed to compare gene expression profiles between the two strains at different temperatures, screening key DEGs associated with high-temperature adaptation, ethanol–acetate metabolism, and cell proliferation. The molecular mechanism underlying high-temperature adaptation of *C. jadinii*

under single ethanol–acetate carbon source conditions was preliminarily clarified. This study provides novel strain resources and technical strategies for the high-temperature adaptive modification of *C. jadinii*, offers a theoretical basis for understanding microbial adaptive regulation under combined high-temperature and composite carbon source stress, and promotes the industrial application of *C. jadinii* in high-temperature fermentation and waste resource recycling, conforming to the development trend of non-conventional yeasts as industrial chassis cells.

2. Materials and Methods

2.1. Microbial Strains

Wild-type *C. jadinii* TU389 with an optimal fermentation temperature of 31 °C and the high-temperature tolerant (37 °C) evolved strain *C. jadinii* X131 obtained after serial-batch-transfer ALE of 131 times were preserved in our laboratory.

2.2. Culture Media

Seed medium (g/L): Glucose 10, yeast extract 3, malt extract 3, peptone 5; natural pH (6.0–6.5), autoclaved at 121 °C for 20 min.

Flask-cultivation medium (g/L): $(NH_4)_2SO_4$ 5, $MgSO_4$ 1, KH_2PO_4 1.5, $CaCl_2$ 0.5, $ZnSO_4 \cdot 7H_2O$ 0.1, $FeSO_4 \cdot 7H_2O$ 0.03, absolute ethanol 6.7, sodium acetate 3.3; pH adjusted to 7.0, autoclaved at 121 °C for 20 min. Ethanol and acetic acid were sterilized by filtration separately and added aseptically after the medium cooled below 50 °C.

Fermenter fermentation medium (g/L): Composite carbon source (ethanol: acetic acid = 2:1, *w*/*w*), with other components consistent with shake-flask medium; pH adjusted to 6.0 with ammonia water. Ethanol and acetic acid were filter-sterilized and added aseptically after medium autoclaving and cooling [4].

Slant preservation medium (g/L): Glucose 20.0, yeast extract 3.0, peptone 5.0, agar 20.0; natural pH, autoclaved at 121 °C for 20 min.

2.3. Serial-Batch-Transfer Adaptive Laboratory Evolution of C. jadinii

Single colonies were picked from preserved slants and inoculated into 50 mL seed medium, cultured at 31 °C and 200 rpm for 18 h to prepare seed liquid. A 10 mL aliquot of seed liquid was inoculated into 100 mL shake-flask fermentation medium and cultured at 37 °C and 200 rpm for 48 h as the 1st transfer of ALE. The ALE process was divided into two stages: 1–27 times of transfer with a 48 h fermentation cycle, and 28–131 times of transfer with a shortened 24 h fermentation cycle to enhance screening pressure. All transfers were performed at a 10.0% (*v*/*v*) inoculation ratio. The strain obtained after serial-batch-transfer ALE of 131 times was named *C. jadinii* X131.

Fermentation broth OD_{600} was measured after each transfer at culture-harvest time point (24 h or 48 h, according to cycle setting), using UV-visible spectrophotometer (Evolution™ 220, Thermo Fisher Scientific (Shanghai) Instruments Co., Ltd., Shanghai, China). Three independent biological replicates were set for each transfer. Mean values and standard deviation were calculated to plot the evolution curve for dynamic biomass monitoring.

2.4. Shake-Flask Fermentation Evaluation of Evolved and Wild-Type Strains

Single colonies of X131 and wild-type TU389 were inoculated into seed medium and cultured at 31 °C and 200 rpm for 18 h. The OD_{600} of seed liquid was standardized to 1.0 for subsequent fermentation. A 5 mL aliquot of standardized seed liquid was inoculated into 50 mL fermentation medium in 250 mL Erlenmeyer flasks. Fermentation was performed at 31 °C and 37 °C respectively, with three biological replicates for each strain-temperature combination, and cultured at 200 rpm for 72 h.

2.5. 5 L Fermenter Scale-Up Fermentation

Standardized seed liquid (200 mL, OD_{600} = 1.0) was prepared for scale-up fermentation. A 5 L fermenter with a working volume of 3 L was used with an inoculation volume of 10.0% (*v*/*v*). Fermentation parameters were set as follows: temperature 31 °C or 37 °C, aeration rate 1.0–1.5 vvm, stirring speed 300–500 rpm, and pH maintained at 6.0 ± 0.2 by automatic supplementation of 2 M HCl or ammonia water. Dissolved oxygen (DO) cascade fed-batch fermentation was adopted, and ethanol–acetate mother liquor (2:1, *w*/*w*) was supplemented based on HPLC-detected carbon source consumption to maintain the total carbon of ethanol–acetate mixture concentration at 5–8 g/L. Three biological replicates were set for each group.

Fermentation broth samples were collected at 0, 12, 24, 30, 36, 48, 51, 58, and 72 h to determine OD_{600} and dry cell weight. Ethanol and acetic acid consumption were quantified to calculate carbon source conversion rate (dry biomass weight/total consumed carbon source weight × 100.0%). After 72 h fermentation, cell pellets were collected by centrifugation (8000 rpm, 10 min) and washed three times with pre-cooled deionized water. Partial samples were used for protein determination, and the remaining samples were frozen at −80 °C for transcriptome sequencing.

2.6. Analytical and Quantification Methods

Ethanol and acetic acid determination: Gas chromatography (GC) was used for quantification according to [22]. A GC instrument (Techcomp, Shanghai, China) equipped with an HP InnoWax capillary column (Agilent, Santa Clara, CA, USA) was applied. Fermentation samples were centrifuged at 8000 rpm and 4 °C for 10 min, and the supernatant was filtered through a 0.22 μm organic filter membrane. GC detection conditions: inlet temperature 200 °C, detector temperature 250 °C; column temperature program: initial 60 °C (1 min), ramp to 100 °C at 10 °C/min (2 min), ramp to 200 °C at 30 °C/min (6 min). Isobutanol was used as the internal standard. Standard curves of ethanol and acetic acid were established for quantitative calculation.

Biomass, protein content, protein yield and conversion-rate determination: All indexes were measured referring to [23]. For biomass determination, 10 mL fermentation broth was centrifuged, washed, and dried to constant weight at 105 °C for dry weight calculation. Lyophilized cell powder (3.2–3.8 mg) was used for nitrogen content detection via Flashsmart elemental analyzer (Thermo Fisher Scientific, Milan, Italy). Protein content was calculated as nitrogen content × 6.25/sample weight, and protein yield (g/L) = biomass × protein content.

To investigate the amino-acid profiles and nutritional characteristics of the evolved strain X131, the cellular amino-acid contents were determined for biomass harvested from cultures grown at 31 °C and 37 °C. Sixteen hydrolyzed amino acids were quantified according to the Chinese National Food Safety Standard GB 5009.124-2016 [24]. Tryptophan and cystine were measured according to reference [25,26]. Total amino acid content (TAA), the ratio of essential amino acids to total amino acids (EAA/TAA), and amino-acid score (AAS) were further calculated based on the FAO/WHO adult essential-amino-acid reference pattern [27].

2.7. Transcriptome Sequencing and Analysis

Transcriptome analysis was performed with minor modifications based on [28]. Four sample groups with three biological replicates each were set as: W-31 (wild-type at 31 °C), W-37 (wild-type at 37 °C), X-31 (evolved strain at 31 °C), and X-37 (evolved strain at 37 °C). Total RNA was extracted using the Trizol method. RNA integrity was detected by 1.0% agarose gel electrophoresis, RNA purity (A260/A280 = 1.8–2.0) was determined by NanoDrop (Thermo Fisher Scientific, Wilmington, DE, USA), and RNA concentration

was quantified by Qubit (Thermo Fisher Scientific, Waltham, MA, USA) to ensure qualified sequencing samples.

Qualified total RNA was used for mRNA enrichment, fragmentation, and cDNA synthesis. After end repair, A-tailing, and adapter ligation, cDNA libraries were constructed via PCR amplification. Library quality was verified using Agilent 2100 (Agilent, Santa Clara, CA, USA) and Qubit (Thermo Fisher Scientific, Waltham, MA, USA) quantification, and qualified libraries were sequenced on the Illumina NovaSeq 6000 platform (PE150) (Illumina, San Diego, CA, USA).

Raw reads were filtered to remove adapter sequences, low-quality reads (Q < 20), and ambiguous reads to obtain clean reads. Clean reads were mapped to the *C. jadinii* reference genome (NCBI Reference Sequence: NW_017963653.1), and transcript assembly and quantification (TPM) were performed using StringTie software (v2.1.1, Center for Computational Biology, Johns Hopkins University, Baltimore, MD, USA). DESeq2 was used for differential expression analysis with screening thresholds of $|\log_2 FC| \geq 1$ and Padj < 0.05. DEGs from three comparison groups (X-37 vs. W-31, X-37 vs. W-37, X-31 vs. W-31) were subjected to GO functional enrichment and KEGG pathway enrichment analysis. All locus tags presented in Table S1 correspond to gene identifiers from this public reference-genome annotation, serve as annotation anchors for transcriptomic data rather than strain-specific genomic identifiers.

2.8. Data Statistical Analysis

All experimental data were presented as mean ± standard deviation (mean ± SD), n = 3 independent biological replicates. Two-way ANOVA (factors: strain, temperature, strain-temperature interaction) was performed using Microsoft® Excel® LTSC-MSO (Version 2408, Build 16.0.17932.21000, Microsoft Corporation, Redmond, WA, USA) for biomass, protein yield and conversion-rate data; one-way ANOVA was applied for other datasets. $p < 0.05$ was considered statistically significant. Transcriptome visualization and enrichment analysis were conducted using R (v4.2.1, R Core Team, Vienna, Austria) language packages (DESeq2, clusterProfiler). Other figures were created in Adobe Photoshop 27.9.1 (Adobe Inc., San Jose, CA, USA).

3. Results

3.1. ALE of Thermotolerant C. jadinii

Wild-type *C. jadinii* with an optimal growth temperature of 31 °C was subjected to serial-batch-transfer ALE 131 times using ethanol and acetic acid as the sole carbon sources. Dynamic monitoring of OD_{600} values showed a three-stage growth pattern: rapid initial increase, medium-term fluctuating optimization, and stable high-level maintenance (Figure 1A). These OD_{600} dynamics indicated that the evolved strain formed genetically stable high-temperature adaptive phenotypes without performance degradation under short-cycle serial transfers.

Shake-flask fermentation results (Figure 1B) showed that the dry biomass of wild-type strain (TU389) was 4.87 g/L at 31 °C (W-31) but decreased by 16.6% to 4.06 g/L at 37 °C (W-37), indicating significant high-temperature growth inhibition. The evolved strain (X131) exhibited slightly increased biomass at 31 °C (X-31, 4.944 g/L, no significant difference vs. W-31) and significantly higher biomass at 37 °C (X-37, 4.478 g/L, 10.4% higher than W-37). The biomass decline rate of the evolved strain at 37 °C was only 9.4%, far lower than that of the wild-type strain, demonstrating expanded temperature adaptation range of the X131 strain.

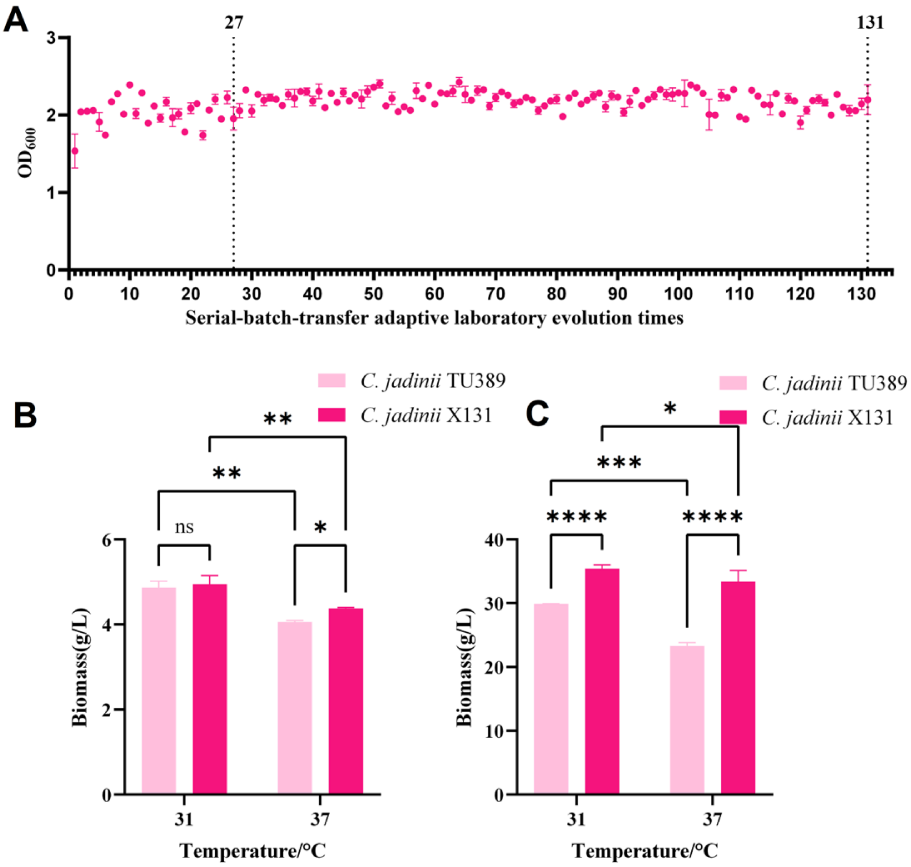


Figure 1. Biomass changes during serial-batch-transfer ALE and fermentation evaluation of the thermotolerant strains. (**A**) OD_{600} variation curve during serial-batch-transfer ALE; (**B**) Shake-flask biomass of *C. jadinii* TU389 and *C. jadinii* X131 at different temperatures; (**C**) 5 L fermenter biomass of *C. jadinii* TU389 and *C. jadinii* X131 at different temperatures. Differences are statistically significant both in terms of strain and temperature effects (two-way ANOVA test). ns: not significant; * $p < 0.05$; ** $p < 0.01$; *** $p < 0.001$; **** $p < 0.0001$.

The 5 L fed-batch fermentation results (Figure 1C) further verified the superior performance of the evolved strain. The wild-type biomass decreased by 22.1% from 29.87 g/L (W-31) to 23.27 g/L (W-37). In contrast, the X131 strain achieved 35.41 g/L biomass at 31 °C (18.5% higher than W-31) and 33.39 g/L at 37 °C (43.4% higher than W-37). From another perspective, the increased biomass of the evolved strain X131 at 31 °C (its original optimal temperature) likely primarily reflects optimized ethanol–acetate utilization. In contrast, biomass at 37 °C maybe arises from the combined effects of enhanced carbon catabolism and acquired thermotolerance in X131.

Fermentation dynamic curves (Figure 2, significance was analyzed in Figure 1C at 72 h) showed that W-31 maintained higher biomass than the wild-type strain after 36 h fermentation, while X-31 gradually outperformed both wild-type groups after 60 h cultivation.

Different from the typical adaptive trade-off of thermotolerant *Saccharomyces cerevisiae* (growth attenuation at ancestral optimal temperature after high-temperature adaptation) reported by Caspeta et al. (2015), the *C. jadinii* X131 in this study achieved bidirectional growth improvement at both 31 °C and 37 °C without obvious fitness trade-off, conferring greater industrial application potential [15].

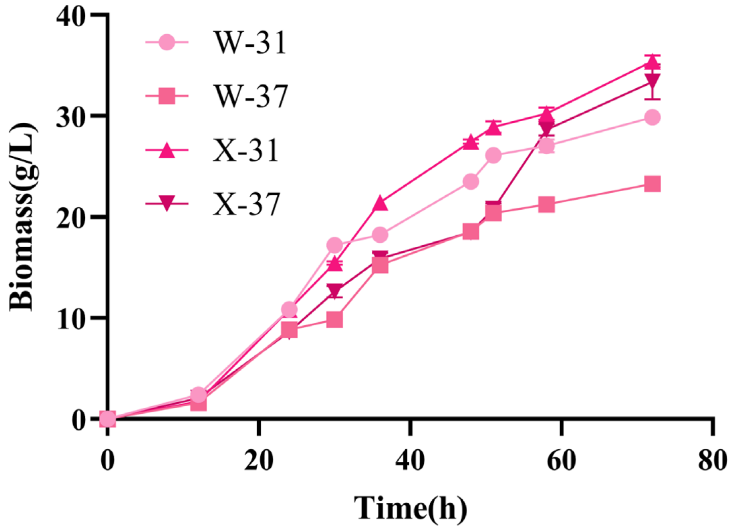


Figure 2. Dynamic biomass curves of evolved and wild-type strains in 5 L fermenters.

Carbon source conversion analysis (Figure 3A) showed that X131 strain possessed significantly higher conversion efficiency than the wild-type strain at both temperatures, with the most prominent improvement in X-37. The cellular protein content of the evolved strain was slightly lower than that of the wild-type strain (Figure 3B) at 37 °C, the superior biomass accumulation contributed to 7.2% and 55.3% higher protein yield in X-31 and X-37 than W-31 and W-37, respectively (Figure 3C). The protein yield of X-31 even exceeded that of X-37, verifying the enhanced production performance of the evolved strain after high-temperature ALE. The results indicated that *C. jadinii* X131 retained and even improved its performance at the ancestral optimal temperature of 31 °C.

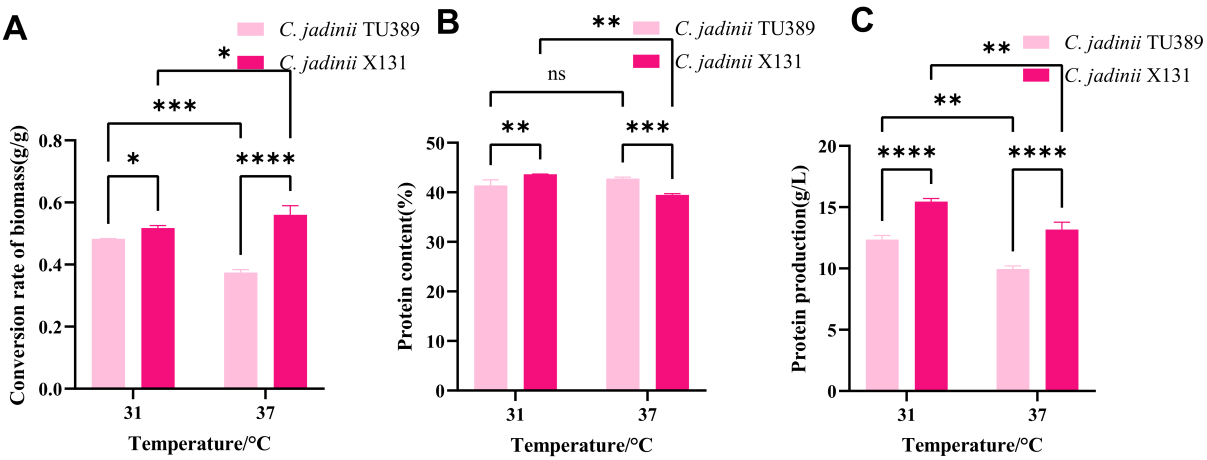


Figure 3. Carbon source conversion rate, protein content and protein yield of different strains at different temperatures in 5 L fermenters. (**A**) Carbon source conversion rate; (**B**) cellular protein content; (**C**) total protein yield. Differences are statistically significant both in terms of strain and temperature effects (two-way ANOVA test). ns: not significant; * $p < 0.05$; ** $p < 0.01$; *** $p < 0.001$; **** $p < 0.0001$.

The p value of the two-way ANOVA test of the interact between temperature and strain was indicated in Table 1. The results revealed trait-dependent fitness modulation in the evolved strain X131, rather than a universal adaptive compromise across all phenotypes. Non-significant strain-by-temperature interaction for biomass in shake-flask experiments indicated consistent growth superiority of X131 at 31 °C and 37 °C under shake-flask batch conditions. Nevertheless, significant strain-temperature interactions for biomass,

carbon-source conversion rate and cellular protein content were detected in fed-batch 5 L bioreactors. This discrepancy between shake-flask and bioreactor datasets can be partly attributed to differences in culture conditions: fed-batch fermentation maintains sustained substrate supply, precise pH control and higher dissolved oxygen levels, which impose distinct metabolic burdens compared with batch shake-flask cultivation.

Table 1. The *p* value of the two-way ANOVA test of the interact between temperature and strain.

		p Value	Significant or Not	Original Data
Shake flask	Biomass	0.1992	No	Figure 1B
5 L Fermenter	Biomass	0.0085	Yes	Figure 1C
	Conversion rate	0.0007	Yes	Figure 3A
	Protein content	0.0019	Yes	Figure 3B
	Protein production	0.7787	No	Figure 3B

Notably, protein yield—the core target metric for single-cell-protein production—exhibited a non-significant strain-by-temperature interaction in 5 L fermenters. This finding demonstrates that X131 retains its advantage in total protein output irrespective of temperature within the tested range, even though the magnitude of biomass and cellular protein-content improvements were temperature-modulated.

Amino acid composition analysis (Table 2) showed that the total amino acid content of X-37 was 36.1 g/100 g, 10.9% lower than X-31 (40.5 g/100 g), indicating that high temperature slightly inhibited total amino acid accumulation. However, no amino acid deficiency was detected in X-37, demonstrating that the evolved strain achieved stable adaptation of amino acid synthesis systems under high temperature after long-term ALE, avoiding the collapse of protein synthesis under thermal stress.

Table 2. Amino acids of X-37 and X-31.

Amino Acids	X-37	X-31
Threonine	2.4	2.6
Valine	2.0	2.2
Methionine	0.6	0.7
Isoleucine	1.6	1.8
Leucine	2.6	2.8
Phenylalanine	1.6	1.7
Lysine	2.4	2.7
Tryptophan	0.4	0.5
Aspartic acid	3.5	3.9
Serine	2.3	2.5
Tyrosine	1.3	1.5
Glutamic acid	6.8	8.1
Glycine	1.6	1.7
Histidine	0.8	1.0
Arginine	2.1	2.3
Proline	1.3	1.4
Alanine	2.2	2.6
Cystine	0.5	0.5
Total amino acid content	36.0	40.5
EAA/TAA (%)	37.8	37.0
Score of relative coefficient (SRC)	79.9	80.6
First-limiting amino acid	Met+Cys	Met+Cys
AAS of first-limiting amino acid (%)	87.3	84.7

The EAA/TAA ratios of X131 at two cultivation temperatures were 36.9% (31 °C) and 37.7% (37 °C), both exceeding the 36.0% threshold for high-quality protein proposed by FAO/WHO [29], indicating that the SCP of X131 possessed excellent basic nutritional properties under both temperature conditions.

Amino acid score (AAS) evaluation based on the FAO/WHO adult reference standard demonstrated that the limiting amino acids of X131 at 31 °C and 37 °C were Met and Cys, which showed the AAS values of 84.7 and 87.3, respectively. The score of relative coefficient (SRC) of X131 at 37 °C (79.9) was almost the same as that at 31 °C (80.6). These results suggest that high-temperature ALE exerts no substantial disturbance on the biosynthetic pathways of essential amino acids, and the protein of the evolved strain retains nutritional value comparable to the parental strain.

Compared with single-carbon-source ALE (glucose, xylose), ethanol–acetate composite carbon source ALE requires coordinated optimization of two sets of carbon transport and metabolic pathways, imposing higher screening pressure but yielding superior carbon utilization efficiency, providing a new strategy for high-temperature ALE of composite carbon source-utilizing microorganisms. Different from the common adaptive trade-off in microbial thermotolerance ALE [15], the evolved strain achieved overall metabolic optimization rather than simple stress resistance compensation, with improved efficiency in carbon transport, energy metabolism, and protein synthesis. This bidirectional optimization phenotype endows the strain with great industrial application value, highlighting the significance of dissecting its global metabolic optimization mechanism.

3.2. Transcriptomic Analysis of the Evolved Strain

3.2.1. Transcriptome Data Quality Evaluation

Strict quality control (QC) was performed on transcriptome sequencing data of W-31, W-37, X-31, and X-37 samples. The raw reads of all samples ranged from 3.90×10^7 to 5.05×10^7, with high consistency between clean reads and raw reads, indicating high data retention rate. The sequencing error rate of all samples was lower than 0.013%, far below the standard threshold ($\leq$0.1%). The Q20 and Q30 ratios exceeded 99.5% and 97.0%, respectively, confirming high sequencing accuracy and reliability. The GC content was stable at 46.7–47.0% without obvious bias or contamination, and the rRNA pollution ratio was controlled below 2.6%, indicating efficient mRNA enrichment. Overall, the transcriptome data was qualified for subsequent analysis.

Principal component analysis (PCA) showed that PC1 and PC2 explained 43.7% and 31.9% of the total variance, respectively, with a cumulative contribution of 75.6%, sufficiently reflecting the overall differences between samples. PCA scatter plot (Figure 4A) showed clear sample grouping: wild-type samples clustered in the negative PC1 region, while evolved strain samples distributed in the positive PC1 region, indicating that strain genotype was the primary factor driving transcriptome variation. Within the same strain, samples cultured at 31 °C and 37 °C were distinctly separated along the PC2 axis, demonstrating that culture temperature was a secondary but significant influencing factor. Tight clustering of biological replicates confirmed good experimental reproducibility. The non-overlapping confidence ellipses of the four groups in the PCA group plot (Figure 4B) further verified that strain type and culture temperature were two independent key variables affecting transcriptome profiles, laying a solid foundation for subsequent differential gene analysis.

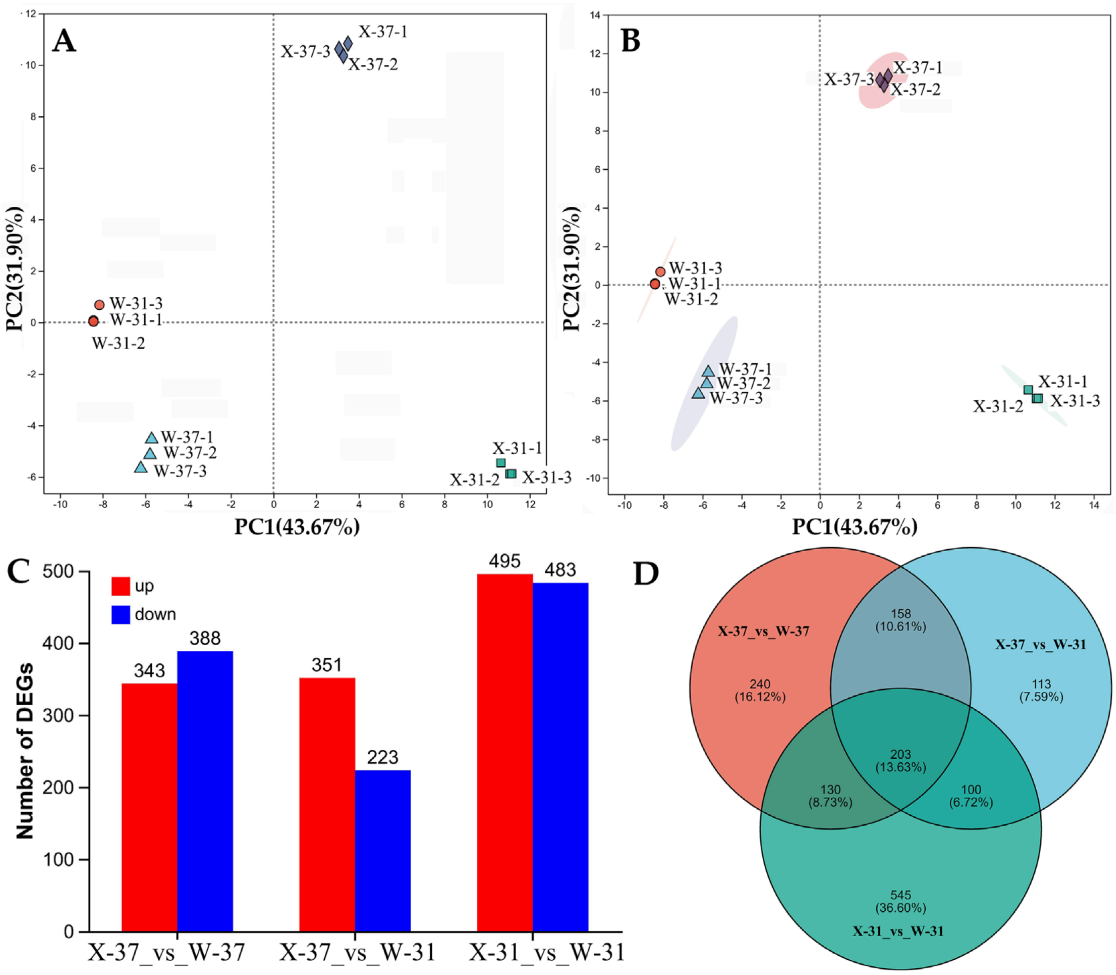


Figure 4. PCA, Differential gene statistics and Venn analysis of transcriptome samples from different strains and temperatures. (**A**) PCA scatter plot; (**B**) PCA grouping plot with confidence ellipses; (**C**) number of DEGs in each comparison group; (**D**) Venn diagram of shared and specific DEGs.

3.2.2. Differential Gene Expression Analysis and Mechanistic Interpretation

Three comparison groups generated abundant differentially expressed genes (DEGs) (Figure 4C): 978 DEGs (495 upregulated, 483 downregulated) in X-31 vs. W-31, 731 DEGs (343 upregulated, 388 downregulated) in X-37 vs. W-37, and 574 DEGs (351 upregulated, 223 downregulated) in X-37 vs. W-31. Volcano plots, Mean-Average (MA) plots, and correlation scatter plots confirmed uniform DEG distribution and high reliability (Figure 5). Venn analysis (Figure 4D) identified 203 core conserved DEGs shared by all three groups, representing key genes for temperature adaptation. Group-specific DEGs indicated distinct regulatory patterns under different conditions.

Long-term high-temperature serial transfer ALE shaped a conserved core regulatory network in the evolved strain, including four synergistic pathways: core metabolic reprogramming, genetic information homeostasis maintenance, oxidative stress defense activation, and metabolic redundancy simplification. All DEGs were classified into eight functional categories. Central carbon metabolism and redox homeostasis, cell cycle and genome maintenance-related pathways, and transmembrane transport system represented the most enriched pathways and core adaptive modules (Figure S1). The major metabolic pathways and gene expression profiles are presented in Figure 6 and Table S1.

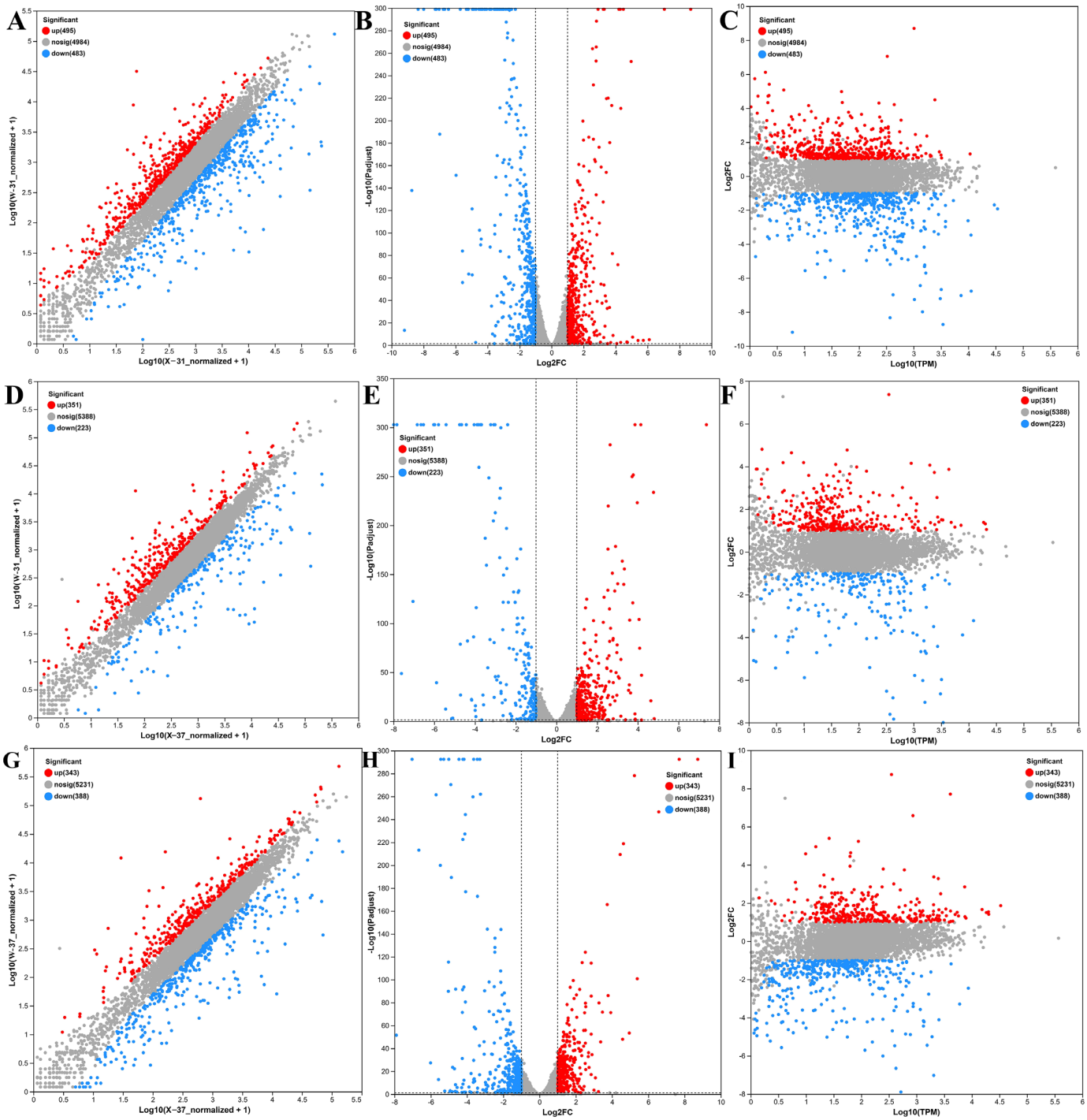


Figure 5. Volcano plots, MA plots and key gene annotation of DEGs in three comparison groups. (**A**) Scatter plot of gene expression correlation for X-31 vs. W-31; (**B**) volcano plot for X-31 vs. W-31; (**C**) MA plot for X-31 vs. W-31; (**D**) scatter plot of gene expression correlation for X-37 vs. W-31; (**E**) volcano plot for X-37 vs. W-31; (**F**) MA plot for X-37 vs. W-31; (**G**) scatter plot of gene expression correlation for X-37 vs. W-37; (**H**) volcano plot for X-37 vs. W-37; (**I**) MA plot for X-37 vs. W-37.

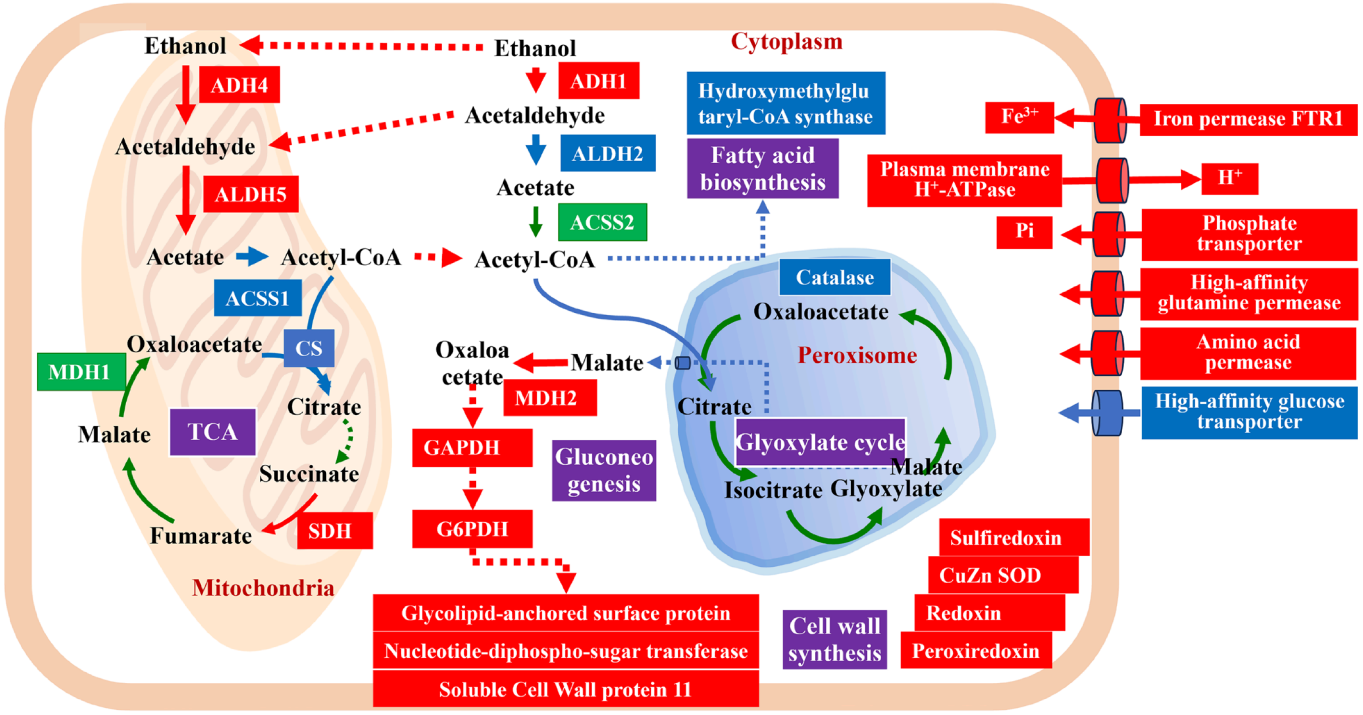


Figure 6. Expression profiles of genes involved in key metabolic pathways of X131, red indicates upregulated genes, blue indicates downregulated genes, green indicates genes with no significant expression difference, and purple represents major metabolic pathways.

- Ethanol Oxidation Pathway Remodeling and Gluconeogenesis Enhancement

Ethanol metabolism is primarily catalyzed by alcohol dehydrogenase, aldehyde dehydrogenase, and acetyl-CoA synthetase, which convert ethanol to acetyl-CoA via intermediate products including acetaldehyde and acetic acid. Transcriptomic and gene sequence analysis revealed that the alcohol dehydrogenases and aldehyde dehydrogenases of *C. jadinii* are mainly localized in the mitochondria and cytoplasm (Table S1 and Figure 6) [4]. In the comparison group of X131 strains fermented at 37 °C (X-37) and wild-type strains fermented at 37 °C (W-37) (Table S1), the expression level of the mitochondrial alcohol dehydrogenase gene (CYBJADRAFT_166331) was significantly upregulated ($Log_2FC = 7.70$) at the transcript level. The expression of cytoplasmic alcohol dehydrogenase (CYBJADRAFT_166331) was also markedly increased ($Log_2FC = 2.11$), with a much higher upregulation magnitude observed in the mitochondrial isoform (Table S1).

Mitochondrial aldehyde dehydrogenase genes (CYBJADRAFT_123321 and CYBJADRAFT_178503) were significantly upregulated ($Log_2FC = 1.65$), whereas the cytoplasmic aldehyde dehydrogenase gene (CYBJADRAFT_191064) was significantly downregulated ($Log_2FC = -1.41$). In the subsequent acetyl-CoA synthesis process, the expression of mitochondrial acetyl-CoA synthetase 1 (CYBJADRAFT_127431) was remarkably downregulated, while no significant change was detected in cytoplasmic acetyl-CoA synthetase 2 (CYBJADRAFT_171467).

Consistent expression regulation patterns of mitochondrial alcohol dehydrogenase (CYBJADRAFT_166331), cytoplasmic alcohol dehydrogenase (CYBJADRAFT_173588), mitochondrial aldehyde dehydrogenase (CYBJADRAFT_178503), mitochondrial acetyl-CoA synthetase 1 (ACS1, CYBJADRAFT_127431), and cytoplasm acetyl-CoA synthetase 2 (CYBJADRAFT_171467) were observed in the comparison groups of X131 at 37 °C (X-37) vs. wild-type at 31 °C (W-31) fermentation and X131 at 31 °C (X-31) vs. wild-type at 31 °C (W-31) fermentation. However, the expression of aldehyde dehydrogenases (CYBJADRAFT_123321) showed no significant differences compared with the control groups.

These results indicate that the main subcellular compartment executing ethanol oxidation is reprogrammed from cytoplasm toward mitochondria, which eliminates the carbonyl toxicity of acetaldehyde in situ and prevents oxidative damage caused by cytoplasmic acetaldehyde accumulation. Previous studies have demonstrated that in fungi utilizing ethanol as a carbon source, the upregulation of mitochondrial isoenzymes, downregulation of cytoplasmic isoenzymes, and transcriptional attenuation of ACS1 represent a universal metabolic reprogramming pattern, which balances energy utilization and thermal stress tolerance [30–32].

Transcriptomic comparison between X131 and wild-type strains cultured at 37 °C revealed significant upregulation of key gluconeogenic enzymes, including glyceraldehyde 3-phosphate dehydrogenase (GAPDH, CYBJADRAFT_165235) and phosphoglycerate mutase (CYBJADRAFT_120520) (Figure 6 and Table S1). Relying on acetyl-CoA generated from ethanol–acetate metabolism, the strain synthesizes endogenous glucose and its metabolites. Additionally, the coordinated upregulation of NAD kinase (NADK, CYBJADRAFT_129771) sustains NADPH production, providing reducing power for the intracellular antioxidant system.

- Rigid Barrier Construction Against Combined Stresses

Under the stress of 37 °C high temperature and ethanol and acetic acid, the cell wall synthesis pathway of X131 strains exhibited significant adaptive upregulation, serving as the core physical barrier against extracellular stresses. In the comparison groups of X-37 vs. W-37 and X-37 vs. X-31, X131 strains showed significant upregulation of cell wall structural protein Wmsu1p (CYBJADRAFT_13824), GH17 family glucosidase SCW11 (CYBJADRAFT_149586), and nucleotide-diphospho-sugar transferase (CYBJADRAFT_167464). In contrast, these proteins showed no significant change or decreased expression under 31 °C fermentation conditions (X-31 vs. W-31) (Table S1).

This suggests that these three proteins synergistically maybe mediate the hydrolysis, branching, and cross-linking of cell wall β-glucan to form a highly compact and rigid cell wall network. This structure effectively reduces the inward penetration of acetic acid molecules and lipid peroxides, alleviates intracellular acidification and oxidative stress, and resists cell lysis induced by high temperature [33–36].

- Intracellular pH Homeostasis

Global reprogramming of the cell membrane transport system is the core mechanism by which X131 strains adapt to acetic acid acidification stress and a key guarantee for their biomass advantage [37]. At set pH 6.0 in fed-batch fermenter, most acetate exists as dissociated anions; nevertheless, a small fraction of undissociated acetic acid can diffuse across plasma membrane and dissociate inside cell, releasing H^+ and triggering cytoplasmic acidification. The gene encoding plasma membrane H^+-ATPase (CYBJADRAFT_128314) was extremely significantly upregulated in X37 strains (Figure 6 and Table S1). This protein maybe continuously pumps intracellular H^+ outward to counteract cytoplasmic acidification caused by diffused undissociated acetic acid and heat-associated metabolic proton generation, acting as the most critical transporter for fungal acetic-acid tolerance. This resolves the core problems of intracellular pH imbalance and inhibited metabolic enzyme activity in wild-type strains at 37 °C [38,39].

- Synergistic Polyamine Synthesis and Toxin Clearance

Significant upregulation of α/β hydrolase family proteins (including FSH1, EAT1 and other isoenzymes) (CYBJADRAFT_189656, CYBJADRAFT_76798, CYBJADRAFT_129113 and CYBJADRAFT_146288) (Table S1) enables compartmentalized clearance of carbonyl toxicants such as acetaldehyde and lipid aldehydes in mitochondria and cytoplasm [40].

Vacuolar acid protease (CYBJADRAFT_120251 and CYBJADRAFT_187587) and RNase T2 (CYBJADRAFT_149172) are synchronously upregulated (Table S1), accelerating the degradation and turnover of heat-denatured proteins and damaged RNA, thereby reducing the accumulation of intracellular toxic substances [41,42].

- Cytoplasmic Antioxidant System Replaces Peroxisomal Function

High temperature and ethanol oxidation produce ROS, driving the formation of a high-temperature-adapted antioxidant network. The cytoplasmic and mitochondrial antioxidant systems were comprehensively upregulated: cytoplasmic soluble antioxidant proteins including peroxiredoxin (CYBJADRAFT_153614), redoxin (CYBJADRAFT_163919), sulfiredoxin (CYBJADRAFT_168838), and copper-zinc superoxide dismutase SOD1 (CYBJADRAFT_177023, partially localized in the mitochondrial intermembrane space to exert functions [43] were significantly upregulated, forming the core intracellular free radical scavenging system [42] (Figure 6). This system utilizes NADPH generated by the pentose phosphate pathway (PPP) as reducing power to eliminate intracellular superoxide anions and lipid peroxides.

In contrast, peroxisomal catalase (CYBJADRAFT_176400) and glutathione S-transferase (CYBJADRAFT_167842) were significantly downregulated, reducing the overall metabolic load of peroxisomes. This alteration alleviates oxidative damage to the peroxisomal membrane and prevents intracellular oxidative stress caused by peroxisome rupture, representing an adaptive strategy of cells under high-temperature stress [44].

- Full-Cycle Activation Sustains Proliferation Under High Temperature

To cope with DNA damage induced by high temperature and accumulated acetaldehyde, multiple genome-stability modules are collectively up-regulated (Figure 7 and Table S1). And five functional modules (S-phase origin firing, DNA synthesis machinery, chromatin remodeling, M-phase segregation, and DNA repair surveillance) are illustrated.

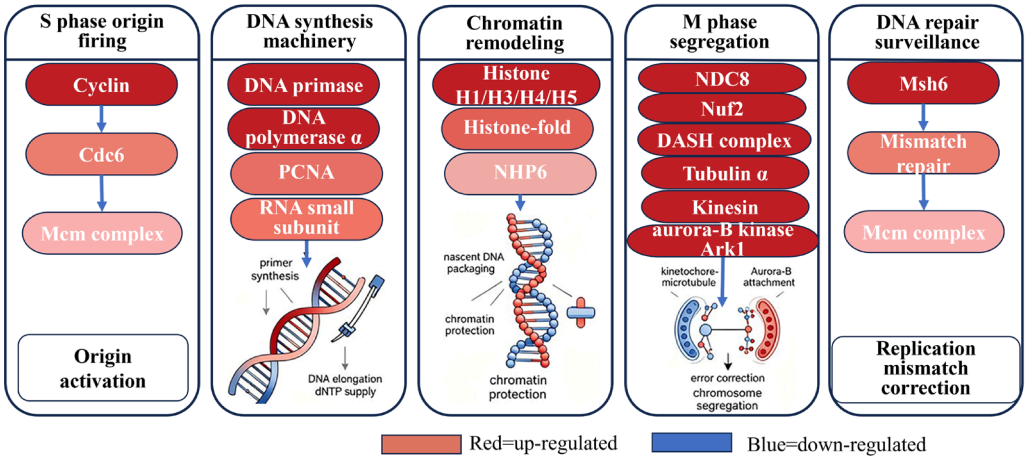


Figure 7. Schematic diagram of DEGs associated with genome-stability-related pathways.

Genes associated with G1/S phase regulation and DNA replication, including the Cyclin family (A/B/D/E-type) (CYBJADRAFT_169288 and CYBJADRAFT_165413), Cdc6 (CYBJADRAFT_167852), proliferating cell nuclear antigen (CYBJADRAFT_126100), MCM replication complex (CYBJADRAFT_177196), and DNA polymerase α (CYBJADRAFT_185097), were significantly upregulated (Figure 7, Table S1), ensuring stable S-phase DNA replication under high temperature [45]. The upregulation of the small subunit of ribonucleotide-diphosphate reductase (CYBJADRAFT_169423) expands the dNTP pool, overcoming the raw material bottleneck of DNA replication under high-temperature conditions [46].

Core kinetochore complexes (NDC80 (CYBJADRAFT_124269), Nuf2 (CYBJADRAFT_190313), DASH complex (CYBJADRAFT_168502)), tubulin (CYBJADRAFT_169067), kinesin (CYBJADRAFT_168352), and Aurora-B kinase (CYBJADRAFT_177620) were significantly upregulated (Figure 7, Table S1). These changes strengthen spindle-chromosome attachment, improve the efficiency of the spindle assembly checkpoint, alleviate high temperature-induced spindle depolymerization and chromosome missegregation, and reduce the proportion of aneuploid cells [47,48].

Significant upregulation of histones (H1/H3/H4) (CYBJADRAFT_133482, CYBJADRAFT_177642, CYBJADRAFT_192701 and CYBJADRAFT_112126), histone-fold proteins (CYBJADRAFT_91363, CYBJADRAFT_151348, CYBJADRAFT_184953, CYBJADRAFT_167229 and CYBJADRAFT_143931), and WD40 scaffold proteins (CYBJADRAFT_166202, CYBJADRAFT_167194, CYBJADRAFT_166137 and CYBJADRAFT_147738) (Figure 7, Table S1) coordinately mediates dynamic chromatin remodeling, compacts chromatin structure, and reduces oxidative damage to exposed DNA [49,50]. The upregulation of DNA mismatch repair protein Msh6 (CYBJADRAFT_178142) inhibits the accumulation of DNA replication errors, ensuring the stable inheritance of thermotolerant traits in X131 strains.

The transcriptomic changes in this pathway directly explain the biomass differences between strains. Wild-type strains exhibit cell cycle arrest at 37 °C, with impaired DNA replication and chromosome segregation leading to blocked cell proliferation and drastically reduced biomass. In contrast, X131 strains activate the complete cell cycle process, unblocking the full G1→S→M cycle and enabling sustainable and high-fidelity proliferation under high temperature. The comprehensive activation of the cell cycle and genomic stability system is the core guarantee for stable proliferation and significantly improved biomass of X131 strains at 37 °C.

In addition, a total of 630 differentially expressed genes without clear functional annotations were identified in this study, including a large number of DUF domain proteins and hypothetical proteins. Among them, 287 genes were significantly upregulated in the X37 vs. W37 comparison group, serving as core candidate targets for subsequent functional verification and novel stress resistance mechanism exploration.

In summary, X131 strains maintain growth advantages at different temperatures via conserved core regulatory mechanisms and respond to temperature-specific stress challenges through unique differential regulation in each group, ultimately achieving full-temperature-range adaptability. This provides a solid molecular basis for the adaptation to temperature fluctuations and efficient production in industrial fermentation.

4. Discussion

Here, we successfully obtained a thermotolerant evolved strain X131 via adaptive laboratory evolution (ALE) under combined ethanol–acetate carbon source and continuous high-temperature stress at 37 °C. Phenotypic characterization in shake flasks and 5 L bioreactors demonstrated that the evolved strain X131 achieved higher biomass and protein production at both 31 °C and 37 °C compared with the wild-type TU389. Notably, no obvious growth trade-off was observed across the two temperatures: the growth advantage of X131 was maintained at both temperatures, which distinguishes this evolved phenotype from many conventional thermotolerant evolved strains [14]. Although slight metabolic rearrangement in amino acid composition was detected under heat stress, the resulting change in total amino acid pool was modest and could be regarded as a minor metabolic cost rather than a fitness trade-off.

Transcriptomic profiling revealed that mitochondrial metabolic reprogramming constitutes a core adaptive mechanism of X131. Upon ALE, ethanol oxidation was partially shifted from the cytoplasm to mitochondria, which facilitates in situ detoxification of cy-

totoxic acetaldehyde. This rearrangement alleviates heat-induced oxidative stress while improving cellular energy supply, jointly supporting efficient utilization of mixed ethanol–acetate carbon sources under high-temperature conditions. Beyond mitochondrial remodeling, multiple intracellular homeostasis systems were transcriptionally coordinated in the evolved strain. Upregulation of H^+-ATPase genes counteract intracellular acidification triggered by acetate [51]; enhanced expression of cell-wall-related genes strengthens cellular resistance to combined heat and weak-acid stress [52]. Meanwhile, cytoplasmic antioxidant networks compensate for the functional limitation of peroxisomes under thermal stress and reduce heat-mediated cellular damage [53].

Consistent with the transcriptional rewiring of metabolism and stress defense, full-cycle activation of genome-stability and cell-cycle pathways was observed in X131 [54]. Genes involved in DNA replication, chromatin remodeling, spindle assembly and DNA damage repair were coordinately upregulated. This transcriptional signature preserves genome integrity and sustains robust cell proliferation at elevated temperature, providing a possible mechanistic explanation for the absence of temperature-dependent growth trade-off in this evolved strain.

X131 exhibits improved biomass and protein production at both the original optimum and elevated temperature, representing a valuable adaptive phenotype. Prior investigations of *C. jadinii* mainly focused on single-carbon-source cultivation without systematic heat-challenge tests or multi-omics dissection of adaptive mechanisms. From an industrial perspective, the phenotype of X131 is attractive for single-cell protein biomanufacturing. The strain tolerates higher fermentation temperature, which reduces cooling consumption during large-scale cultivation [55]. Moreover, it can valorize waste streams containing ethanol and acetate. The cellular protein produced by X131 possesses well-balanced amino acid profiles, further supporting its application potential as a single-cell protein.

The proposed adaptive mechanism is mainly inferred from transcriptomic data; whole-genome resequencing and ploidy analysis are required to pinpoint the underlying genetic variations. Future work will include whole-genome sequencing, ploidy measurement validation of key differentially expressed genes. Pilot-scale fermentation will also be performed to evaluate the long-term operational stability of X131 for industrial single-cell protein production.

Supplementary Materials: The following supporting information can be downloaded at https://www.mdpi.com/article/10.3390/fermentation12100480/s1, Figure S1: GO enrichment analysis of DEGs in three comparison groups; Table S1: Log_2FC values of key differentially expressed genes involved in carbon metabolism, stress response, cell-cycle and chromatin remodeling.

Author Contributions: Conceptualization, L.C.; B.Y., G.C. and D.L.; methodology, L.C., L.L., X.L., Y.C. and B.L.; software, L.C. and W.B.; validation, L.C. and L.L.; formal analysis, X.L. and Y.C.; investigation, L.C., L.L., Y.C. and W.B.; resources, Y.C. and X.L.; data curation, L.C. and B.L.; writing—original draft preparation, L.C.; writing—review and editing, D.L., B.Y., G.C. and W.B.; visualization, B.L.; supervision, B.Y., G.C., B.Y. and D.L.; project administration, D.L., G.C., B.Y. and W.B.; funding acquisition, L.C. All authors have read and agreed to the published version of the manuscript.

Funding: This research was funded by the National Key Research and Development Program of MOST of China, grant number 2024YFA0918103 and Central-Guided Local Science and Technology Development Fund Project (Tianjin), grant number 25ZYCGYS00230.

Institutional Review Board Statement: Not applicable.

Informed Consent Statement: Not applicable.

Data Availability Statement: All relevant data are available from the corresponding author upon reasonable request.

Conflicts of Interest: The authors declare no conflicts of interest.

Abbreviations

The following abbreviations are used in this manuscript:

ALE	Adaptive laboratory evolution
ROS	Reactive oxygen species
EAA	Essential amino acids
TAA	Total amino acids
AAS	Amino-acid score
SRC	Score of relative coefficient
QC	Quality control
PCA	Principal component analysis
DEGs	Differentially expressed genes
MA	Mean-Average
ACS1	Acetyl-CoA synthetase 1

References

1. Buerth, C.; Tielker, D.; Ernst, J.F. *Candida utilis* and *Cyberlindnera (Pichia) jadinii*: Yeast relatives with expanding applications. *Appl. Microbiol. Biotechnol.* **2016**, *100*, 6981–6990. [CrossRef] [PubMed]
2. Gu, L.; Zhang, R.; Fan, X.; Wang, Y.; Ma, K.; Jiang, J.; Li, G.; Wang, H.; Fan, F.; Zhang, X. Development of CRISPR/Cas9-based genome editing tools for polyploid yeast *Cyberlindnera jadinii* and its application in engineering heterologous Steroid-Producing Strains. *ACS Synth. Biol.* **2023**, *12*, 2947–2960. [CrossRef] [PubMed]
3. Villarreal, P.; Molinet, J.; Braun-Galleani, S.; Cubillos, F.A. Non-Conventional yeasts as a source of genetic diversity and biotechnological potential. *Annu. Rev. Microbiol.* **2025**, *79*, 595–614. [CrossRef] [PubMed]
4. Cao, Y.; Ma, L.; Li, Y.; Zhu, Z.; Duan, Y.; Bai, W.; Long, L.; Shi, P.; Chen, L.; Li, D. Enhanced biomass and protein synthesis in engineered *Cyberlindnera jadinii* growing on ethanol/acetate: Metabolic engineering and transcriptomic mechanism. *Foods* **2026**, *15*, 1464. [CrossRef] [PubMed]
5. Feng, T.; Yu, H.; Ye, L. Mechanisms and strategies for engineering oxidative stress resistance in *Saccharomyces cerevisiae*. *Chem. Bio Eng.* **2025**, *2*, 409–422. [CrossRef] [PubMed]
6. Lemmel, S.A.; Heimsch, R.C.; Edwards, L.L. Optimizing the continuous production of *Candida utilis* and *Saccharomycopsis fibuliger* on potato processing wastewater. *Appl. Environ. Microbiol.* **1979**, *37*, 227–232. [CrossRef] [PubMed]
7. Triboli, E.P.D.R.; Jurkiewicz, C.H.; Borzani, W. Influence of the temperature on batch cultivation of Candida utilis IZ-1840 on a synthetic medium containing glycerol as the main carbon source. *Biotechnol. Lett.* **1994**, *16*, 385–388. [CrossRef]
8. Calderón, R.R.; Boza, F.A.; Benmites-Alfaro, E.; Gómez, O.T.; Flores, J.C. Consortium of *Candida utilis*, *Kluyveromyces marxianus* and *Saccharomyces cerevisiae* yeasts for vinasse fermentation of *Agave americana* L. Liquor for biomass production and reduction in chemical oxygen demand. *Fermentation* **2025**, *11*, 281. [CrossRef]
9. Khalid, H.; Amin, F.R.; Gao, L.; Chen, L.; Chen, W.; Javed, S.; Li, D. Syngas conversion to biofuels and biochemicals: A review of process engineering and mechanisms. *Sustain. Energy Fuels* **2024**, *8*, 9–28. [CrossRef]
10. Zhai, Y.; Chen, L.; Ma, L.; Duan, Y.; Chen, W.; Long, L.; Wang, G.; Shi, A.; Chen, G.; Li, D. Fluorescent protein-based anaerobic reporter for construction of promoter libraries in *Clostridium autoethanogenum*. *Int. J. Biol. Macromol.* **2025**, *310*, 143155. [CrossRef] [PubMed]
11. Zhai, Y.; Chen, L.; Liu, F.; Li, F.; Long, L.; Chi, M.; Ma, J.; Chen, W.; Yang, Y.; Duan, Y.; et al. Engineering energy-robust *Clostridium autoethanogenum* via integrated nanotechnology and transcription-guided metabolic reprogramming. *Trends Biotechnol.* **2026**, *online first*. [CrossRef] [PubMed]
12. Li, J.; Luo, X.; Liu, H.; Zhang, X.; Tan, H.; Xiong, X. Carbon chain elongation microorganism stimulates caproate production from ethanol and acetate under applied voltage regulation. *Front. Microbiol.* **2025**, *16*, 1597990. [CrossRef] [PubMed]
13. Allaart, M.T.; Fox, B.B.; Nettersheim, I.; Pabst, M.; Sousa, D.Z.; Kleerebezem, R. Physiological and stoichiometric characterization of ethanol-based chain elongation in the absence of short-chain carboxylic acids. *Sci. Rep.* **2023**, *13*, 17370. [CrossRef] [PubMed]
14. Hermansen, C.; Siao, R.; Chua, G.G.; Lee, M.R.X.; Thong, A.; Weingarten, M.; Lindley, N.; Peterson, E.C. Short-chain fatty acid utilization in *Cyberlindnera jadinii* for single-cell protein and odd-chain fatty acid production. *Microorganisms* **2025**, *13*, 1558. [CrossRef] [PubMed]
15. Caspeta, L.; Nielsen, J. Thermotolerant yeast strains adapted by laboratory evolution show trade-off at ancestral temperatures and preadaptation to other stresses. *mBio* **2015**, *6*, e00431. [CrossRef] [PubMed]

16. Caspeta, L.; Chen, Y.; Nielsen, J. Thermotolerant yeasts selected by adaptive evolution express heat stress response at 30 °C. *Sci. Rep.* **2016**, *6*, 27003. [CrossRef] [PubMed]
17. Kieliszek, M.; Bierla, K.; Jiménez-Lamana, J.; Kot, A.M.; Alcántara-Durán, J.; Piwowarek, K.; Błażejak, S.; Szpunar, J. Metabolic response of the yeast *Candida utilis* during enrichment in Selenium. *Int. J. Mol. Sci.* **2020**, *21*, 5287. [CrossRef] [PubMed]
18. Liu, L.; Liu, F.; Yan, Z.; Zhou, H.; Song, W. Transcriptome analysis of damage mechanism of *Candida utilis* under U(VI) stress. *Mar. Pollut. Bull.* **2023**, *196*, 115650. [CrossRef] [PubMed]
19. He, Q.; Gong, G.; Wan, T.; Hu, H.; Yu, P. An integrated transcriptomic and metabolic phenotype analysis to uncover the metabolic characteristics of a genetically engineered *Candida utilis* strain expressing δ-zein gene. *Front. Microbiol.* **2023**, *14*, 1241462. [CrossRef] [PubMed]
20. Dong, D.; Yan, Y.; Yang, F.; Yao, H.; Li, Y.; Huang, X.; Aihemaiti, M.; Zhan, F.; Hou, M.; Cui, W. Integrated microbiota and metabolomics analysis of *Candida utilis* CU-3 solid-state fermentation effects on cottonseed hull-Based feed. *Microorganisms* **2025**, *13*, 1380. [CrossRef] [PubMed]
21. Wu, J.; Ohnuki, S.; Teyssonnière, É.; Yasukawa, T.; Masuo, N.; Schacherer, J.; Ohya, Y. Genetic and phenotypic insights into *Cyberlindnera jadinii* as a promising yeast for industrial biotechnology. *G3 Genes Genomes Genet.* **2025**, *15*, jkaf145. [CrossRef] [PubMed]
22. Tong, S.; Chen, W.; Hong, R.; Chai, M.; Sun, Y.; Wang, Q.; Li, D. Efficient mycoprotein production with low CO_2 emissions through metabolic engineering and fermentation optimization of *Fusarium venenatum*. *J. Agric. Food Chem.* **2024**, *72*, 604–612. [CrossRef] [PubMed]
23. Hong, R.; Tong, S.; Chai, M.; Chen, W.; Liu, X.; Chen, Y.; Li, D. Enhancing mycoprotein yield: Metabolic modulation of chitin synthase in *Fusarium venenatum*. *J. Agric. Food Chem.* **2024**, *72*, 27274–27283. [CrossRef] [PubMed]
24. Zhang, Y.; Sun, S.; Li, Y.; Han, X.; Liu, C.; Zhu, W. Analysis of flesh content, muscle nutritional components and quality of crayfish Farmed in paddy fields in major breeding provinces of China. *Foods* **2026**, *15*, 2277. [CrossRef] [PubMed]
25. Weber, P. Determination of amino acids in food and feed by microwave hydrolysis and UHPLC-MS/MS. *J. Chromatogr. B* **2022**, *1209*, 123429. [CrossRef] [PubMed]
26. Ning, J.; Chen, J.; Liu, W.; Chen, X.; Luo, X.; Yue, X. Characterization and nutrition assessment of amino acids in different domains between donkey colostrum and mature milk. *J. Food Compos. Anal.* **2024**, *132*, 106345. [CrossRef]
27. Li, C.; Wang, M.; Li, H.; Li, H.; Yu, J. Amino acid profile modulates gastrointestinal digestion and potential bioactive peptide release in liquid infant formula: An in vitro study. *Food Res. Int.* **2026**, *245*, 120633. [CrossRef]
28. Chen, L.; Tong, S.; Liu, W.; Zhang, Y.; Khalid, H.; Long, L.; Li, Y.; Li, D.; Yan, B.; Chen, G. Electroporation-induced mutation and transcriptome analysis for high DHA production in Schizochytrium limacinum GCD2032. *Algal Res.* **2023**, *76*, 103297. [CrossRef]
29. Millward, D.J. Amino acid scoring patterns for protein quality assessment. *Br. J. Nutr.* **2012**, *108*, S31–S43. [CrossRef] [PubMed]
30. Boubekeur, S.; Camougrand, N.; Bunoust, O.; Rigoulet, M.; Guérin, B. Participation of acetaldehyde dehydrogenases in ethanol and pyruvate metabolism of the Yeast *Saccharomyces cerevisiae*. *Eur. J. Biochem.* **2001**, *268*, 5057–5065. [CrossRef] [PubMed]
31. Gutiérrez-Corona, J.F.; González-Hernández, G.A.; Padilla-Guerrero, I.E.; Olmedo-Monfil, V.; Martínez-Rocha, A.L.; Patiño-Medina, J.A.; Meza-Carmen, V.; Torres-Guzmán, J.C. Fungal alcohol dehydrogenases: Physiological function, molecular properties, regulation of their production, and biotechnological potential. *Cells* **2023**, *12*, 2239. [CrossRef] [PubMed]
32. Liboro, K.; Yu, S.-R.; Lim, J.; So, Y.-S.; Bahn, Y.-S.; Eoh, H.; Park, H. Transcriptomic and metabolomic analysis revealed roles of Yck2 in carbon metabolism and morphogenesis of *Candida albicans*. *Front. Cell. Infect. Microbiol.* **2021**, *11*, 636834. [CrossRef] [PubMed]
33. Gastebois, A.; Aimanianda, V.; Bachellier-Bassi, S.; Nesseir, A.; Firon, A.; Beauvais, A.; Schmitt, C.; England, P.; Beau, R.; Prévost, M.C.; et al. SUN proteins belong to a novel family of β-(1,3)-glucan-modifying enzymes involved in fungal morphogenesis. *J. Biol. Chem.* **2013**, *288*, 13387–13396. [CrossRef] [PubMed]
34. Wen, T.; Qian, Z.; Sun, L.; Cui, F.; Zan, X.; Meng, L.; Sun, W. Fungal β-1, 3-glucanosyltransferases: A comprehensive review on classification, catalytic mechanism and functional role. *Int. J. Biol. Macromol.* **2025**, *289*, 138651. [CrossRef] [PubMed]
35. Lesage, G.; Bussey, H. Cell wall assembly in *Saccharomyces cerevisiae*. *Microbiol. Mol. Biol. Rev.* **2006**, *70*, 317–343. [CrossRef] [PubMed]
36. Kawahata, M.; Masaki, K.; Fujii, T.; Iefuji, H. Yeast genes involved in response to lactic acid and acetic acid: Acidic conditions caused by the organic acids in *Saccharomyces cerevisiae* cultures induce expression of intracellular metal metabolism genes regulated by Aft1p. *FEMS Yeast Res.* **2006**, *6*, 924–936. [CrossRef] [PubMed]
37. Guaragnella, N.; Bettiga, M. Acetic acid stress in budding yeast: From molecular mechanisms to applications. *Yeast* **2021**, *38*, 391–400. [CrossRef] [PubMed]
38. Kane, P.M. Proton transport and pH control in fungi. *Adv. Exp. Med. Biol.* **2016**, *892*, 33–68. [CrossRef] [PubMed]
39. Salas-Navarrete, P.C.; Rosas-Santiago, P.; Suárez-Rodríguez, R.; Martínez, A.; Caspeta, L. Adaptive responses of yeast strains tolerant to acidic pH, acetate, and supraoptimal temperature. *Appl. Microbiol. Biotechnol.* **2023**, *107*, 4051–4068. [CrossRef] [PubMed]

40. Madeo, F.; Engelhardt, S.; Herker, E.; Lehmann, N.; Maldener, C.; Proksch, A.; Wissing, S.; Fröhlich, K.-U. Apoptosis in yeast: A new model system with applications in cell biology and medicine. *Curr. Genet.* **2002**, *41*, 208–216. [CrossRef] [PubMed]
41. Hecht, K.A.; O'Donnell, A.F.; Brodsky, J.L. The proteolytic landscape of the yeast vacuole. *Cell Logist.* **2014**, *4*, e28023. [CrossRef] [PubMed]
42. Devenish, R.J.; Klionsky, D.J. Autophagy: Mechanism and physiological relevance 'brewed' from yeast studies. *Front. Biosci. (Sch. Ed.)* **2012**, *4*, 1354–1363. [CrossRef] [PubMed]
43. Sturtz, L.A.; Diekert, K.; Jensen, L.T.; Lill, R.; Culotta, V.C. A fraction of yeast Cu,Zn-superoxide dismutase and its metallochaperone, CCS, localize to the intermembrane space of mitochondria: A physiological role for SOD1 in guarding against mitochondria. *J. Biol. Chem.* **2001**, *276*, 38084–38089. [CrossRef] [PubMed]
44. Sibirny, A.A. Yeast peroxisomes: Structure, functions and biotechnological opportunities. *FEMS Yeast Res.* **2016**, *16*, fow038. [CrossRef] [PubMed]
45. Sclafani, R.A.; Holzen, T.M. Cell cycle regulation of DNA replication. *Annu. Rev. Genet.* **2007**, *41*, 237–280. [CrossRef] [PubMed]
46. Chabes, A.; Georgieva, B.; Domkin, V.; Zhao, X.; Rothstein, R.; Thelander, L. Survival of DNA damage in yeast directly depends on increased dNTP levels allowed by relaxed feedback inhibition of ribonucleotide reductase. *Cell* **2003**, *112*, 391–401. [CrossRef] [PubMed]
47. Wei, R.R.; Sorger, P.K.; Harrison, S.C. Molecular organization of the Ndc80 complex, an essential kinetochore component. *Proc. Natl. Acad. Sci. USA* **2005**, *102*, 5363–5367. [CrossRef] [PubMed]
48. Ng, C.T.; Deng, L.; Chen, C.; Lim, H.H.; Shi, J.; Surana, U.; Gan, L. Electron cryotomography analysis of Dam1C/DASH at the kinetochore-spindle interface in situ. *J. Cell Biol.* **2019**, *218*, 455–473. [CrossRef] [PubMed]
49. Lei, Y.; Huang, Y.; Wen, X.; Yin, Z.; Zhang, Z.; Klionsky, D.J. How cells deal with the fluctuating environment: Autophagy regulation under stress in yeast and mammalian systems. *Antioxidants* **2022**, *11*, 304. [CrossRef] [PubMed]
50. Wu, J.; Shang, J.; Zhao, L.; Fu, X.; Lv, J.; Lv, S.; Xv, C.; Jin, W.; Lv, J.; Ma, F.; et al. Unraveling histones: Plant protectors under environmental stress unlocking the key to resilience. *Plant Soil* **2025**, *516*, 1227–1256. [CrossRef]
51. Pittman, J.K. Multiple transport pathways for mediating intracellular pH homeostasis: The contribution of H^+/ion exchangers. *Front. Plant Sci.* **2012**, *3*, 18495. [CrossRef] [PubMed]
52. Azegami, C.; Ohta, M.; Wannarat, P.; Fujimura, T. Study on gene expression mechanism of cell wallrelated gene under abiotic stress. *Plant Cell Physiol.* **2007**, *48*, 855. [CrossRef]
53. Tartik, M. Yeast stress response to synthetic constructs. *ACS Synth. Biol.* **2026**, *15*, 368–386. [CrossRef] [PubMed]
54. Skoneczna, A.; Kaniak, A.; Skoneczny, M. Genetic instability in budding and fission yeast-sources and mechanisms. *Fems Microbiol. Rev.* **2015**, *39*, 917–967. [CrossRef] [PubMed]
55. Abdel-Banat, B.M.A.; Hoshida, H.; Ano, A.; Nonklang, S.; Akada, R. High-temperature fermentation: How can processes for ethanol production at high temperatures become superior to the traditional process using mesophilic yeast? *Appl. Microbiol. Biotechnol.* **2010**, *85*, 861–867. [CrossRef] [PubMed]

Disclaimer/Publisher's Note: The statements, opinions and data contained in all publications are solely those of the individual author(s) and contributor(s) and not of MDPI and/or the editor(s). MDPI and/or the editor(s) disclaim responsibility for any injury to people or property resulting from any ideas, methods, instructions or products referred to in the content.